Lithospheric structure under the western African-European plate boundary : a transect across the Atlas Mountains and the Gulf of Cadiz

H. Zeyen, P. Ayarza, M. Fernandez, A. Rimi

TECTONICS, VOL. 24, TC2001, doi:10.1029/2004TC001639, 2005

Lithospheric structure under the western African-European plate boundary: A transect across the Atlas Mountains and the Gulf of Cadiz

Hermann Zeyen

Département des Sciences de la Terre, UMR 8148 IDES, Université Paris-Sud, Orsay, France

Puy Ayarza

Facultad de Ciencias, Departamento de Geologia, Universidad de Salamanca, Salamanca, Spain

Manel Fernàndez

Group of Dynamics of the Lithosphere, Institute of Earth Sciences "Jaume Almera," Consejo Superior de Investigaciones Científicas (CSIC), Barcelona, Spain

Abdelkrim Rimi

Scientific Institute, Department of Earth Physics, Rabat-Agdal, Morocco

Received 23 February 2004; revised 25 October 2004; accepted 17 December 2004; published 5 March 2005.

[1] We present a two-dimensional lithospheric thermal and density model along a transect running from the southwestern Iberian Peninsula to the northwestern Sahara. The main goal is to investigate the lithosphere structure underneath the Gulf of Cadiz and the Atlas Mountains. The model is based on the assumption of topography in local isostatic equilibrium and is constrained by surface heat flow, gravity anomalies, geoid, and topography data. The crustal structure has been constrained by seismic and geological data where available. Mantle density is supposed to vary linearly with temperature, providing the link between thermal and density-related data. The lithospheric thickness varies strongly along the profile, going from near 100 km under the Iberian Peninsula to at least 160–190 km under the Gulf of Cadiz and the Gharb foreland basin in Morocco and to 70 km underneath the Atlas Mountains, coinciding with a region of Neogene volcanism. The thickening of the lithosphere is interpreted as a SW trending lithospheric slab extending from the western Betics to the Gulf of Cadiz and the Gharb Basin, whereas the thin lithosphere underneath the Atlas may be interpreted as plume-like asthenospheric upwelling similar to those observed in the west European Alpine foreland or as a side effect of a slab penetrating the less viscous asthenosphere. **Citation:** Zeyen, H., P. Ayarza, M. Fernàndez, and A. Rimi (2005), Lithospheric structure under the western African-European plate boundary: A transect across the Atlas Mountains and the Gulf of Cadiz, *Tectonics*, *24*, TC2001, doi:10.1029/2004TC001639.

0278-7407/05/2004TC001639

1. Introduction

[2] The deep structure of the plate boundary between the African and European plates has long been a matter of debate, particularly in the region of the Atlantic-Mediterranean transition. In a limited area, the convergence between the two plates has produced very different structures: the subsiding Alboran Basin surrounded by a narrow arc-shaped thrust belt extending in EW direction through the Betic orogen in the north and the Rif mountains in the south with its apex at the Gibraltar Strait (Figure 1); the intraplate Atlas Mountains with a topography exceeding the one expected from the estimated shortening; and finally, a possible subducting slab or delaminated mantle lithosphere under the Gulf of Cadiz beneath the Gibraltar arc. All these areas are affected by shallow, medium deep and even deep seismic activity [*Buforn and Coca*, 2002; *Hatzfeld and Frogneaux*, 1981; *López Casado et al.*, 2001; *Ramdani*, 1998].

[3] Many studies have focused on the structure of the Alboran Basin and its transition to the Betics and the Rif Mountains: seismic reflection and refraction profiling [e.g., *Banda et al.*, 1993; *Comas et al.*, 1997; *Hatzfeld et al.*, 1978], seismic tomography [*Bijwaard et al.*, 1998; *Blanco and Spakman*, 1993; *Calvert et al.*, 2000; *Seber et al.*, 1996b], gravity modeling [*Torné and Banda*, 1992; *Torné et al.*, 2000; *Watts et al.*, 1993], magnetic [*Galdeano et al.*, 1974] and heat flow [*Polyak et al.*, 1996; *Rimi et al.*, 1998] studies agree in a thin crust and lithosphere under the central east Alboran Basin, thickening rapidly toward the arc-shaped orogenic belt.

[4] West of the Gibraltar arc, several studies concerned the deep structure of the African-Eurasian plate transition from the Eastern Atlantic oceanic domain to the continental Iberian and Moroccan margins. Seismic [e.g., *Banda et al.*, 1995; *González et al.*, 1998; *Gutscher et al.*, 2002; *Maldonado et al.*, 1999; *Sartori et al.*, 1994; *Zitellini et*

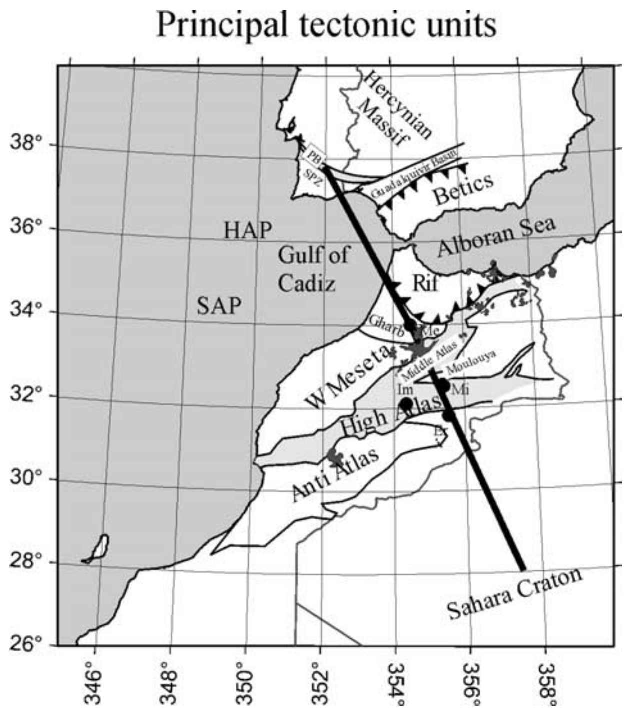

Figure 1. Principal tectonic units crossed by the profile (thick black line). Dark gray irregular spots in Morocco locate Neogene volcanic activity (simplified from *Service Géologique du Maroc*, 1985]). Abbreviations are as follows: PB, Pyrite Belt; SPZ, South Portuguese Zone. Town abbreviations are as follows: Er, Er-Rachidia; HAP, Horseshoe Abyssal Plane; Im, Imilchil; Me, Meknes; Mi, Midelt; SAP, Seyne Abyssal Plane. See color version of this figure in the HTML.

al., 2001], gravity [*González et al.*, 1996; *Gràcia et al.*, 2003], magnetic [*Dañobeitia et al.*, 1999; *Srivastaba et al.*, 1990], and heat flow [*Fernàndez et al.*, 1998; *Rimi*, 1999; *Rimi et al.*, 1998] analyses show that both the crust and the lithospheric mantle, thin toward the central and distal parts of the Gulf of Cadiz region though the crustal nature, continental versus oceanic, is a debatable question.

[5] Recent deep seismic reflection data and integrated lithospheric models [*Carbonell et al.*, 2003; *Fernàndez et al.*, 2004; *Simancas et al.*, 2003] across the south Variscan Iberian Massif have permitted to image the deep structure of the Iberian mainland adjacent to the Gulf of Cadiz margin. However, details on the structure across the North African margin toward the stable Sahara domain are scarcer. Seismic data and recent structural studies [*Teixell et al.*, 2003] suggest that the crust underneath the High Atlas presents very little shortening and is too thin as to isostatically compensate the elevated topography of this orogen. Seismicity and tomography studies reveal a lithospheric thinning in the Middle and High Atlas as well as in the Alboran basin whereas a lithospheric root has been proposed beneath the Gibraltar arc [*Calvert et al.*, 2000; *Seber et al.*, 1996b].

[6] In summary, previous studies show that crust and lithospheric mantle thin from the Betic-Rif orogenic belt to the inner parts of the Gibraltar arc. However, there is little knowledge about how the lithosphere evolves to the outer parts of the arc, mainly toward the Atlantic oceanic domain and the stable Sahara Craton where tomography studies loose resolution at crustal and uppermost mantle levels, because of the poor coverage of seismic stations.

[7] In this paper, we integrate heat flow, geoid, gravity and topography data on a NNW-SSE, 1200 km long transect that starts in the southwestern Variscan Iberian Massif on the Eurasian plate, crosses the Gulf of Cadiz, the Rif foreland, and the Middle and High Atlas and ends in the Sahara Craton (Figure 1). The aim of this work is to develop a lithospheric model that explains the deep structure underneath this plate boundary region, aiding to understand the way the crust and lithospheric mantle accommodated deformation beneath the Gulf of Cadiz and the Atlas Mountains. The results are discussed in terms of possible constraints on proposed geodynamic models to explain the Cenozoic evolution of the region.

2. Geological and Geophysical Context

[8] For the sake of simplicity, we have divided the study region in two domains: the Gulf of Cadiz domain, including both, the south Iberian and the northwest Moroccan continental margins, and the adjacent mainlands (the South Portuguese Zone and the Gharb Basin, respectively); and the Atlas-Sahara domain, which includes the Moroccan Meseta, the Atlas Mountains, and the Anti-Atlas and Sahara Platform.

2.1. Gulf of Cadiz Domain

[9] The Gulf of Cadiz separates the Iberian and African mainlands through a marine region 350–400 km wide, which encompasses the boundary between both plates. From its eastern limit at the Gibraltar strait, the Gulf of Cadiz deepens progressively to the center and west, where it opens to the Atlantic oceanic domain.

[10] The tectonic evolution of the Gulf of Cadiz region is related to the opening of the Central and North Atlantic and to the relative motion between Iberia and Africa [e.g., *Klitgord and Schouten*, 1986; *Malod and Mauffret*, 1990; *Srivastaba et al.*, 1990]. Continental breakup started at the central African margin in the Triassic and propagated to the north until middle Late Jurassic times producing seafloor spreading in the northwestern African margin and a transtensive tectonic regime between Africa and Iberia/Newfoundland. The separation between the Iberian and the North American plates happened at chron M0 (118 Ma) whereas convergence between Eurasia and Africa started at chron 31 (70 Ma). Iberia moved together with the African plate between latest Cretaceous and mid-Eocene (chron 19, 42 Ma), when it started to move as an independent plate and a new plate boundary was formed in the Azores-Gibraltar Fracture Zone. The sense of motion between Africa and Iberia/Eurasia has remained essentially the same since that time producing contemporaneous transtension near the Azores and transpression in the Gulf of Cadiz. The convergence between Africa and Eurasia

produced, farther to the east, the closure of the Tethys Ocean and a collisional orogenic chain. During the late Oligocene-early Miocene, this orogen rifted and disrupted, initiating the formation of the Western Mediterranean and producing the lateral expulsion of the Alboran domain. Close to the apex of the Gibraltar arc, the Alboran domain has overthrust deformed Mesozoic and Tertiary sequences of the South Iberia and North Africa paleomargins. Stacking of these external units during the early middle Miocene caused the formation of the Guadalquivir and Gharb foreland basins. On the other hand, the structural units forming the Betic and Rif chains have their continuation beneath the Gulf of Cadiz. All these units are overlying a Hercynian basement that gently dips toward the East in the Gulf of Cadiz and toward the South and North beneath the Betics and Rif, respectively.

[11] In the past 20 years, a number of studies have been conducted to unravel the deep structure of the south Iberian continental margins and its transition to the northern African margins. The results of these studies show that crustal thickness gently decreases from $\sim$30–32 km in the Iberian and Moroccan mainlands to <25 km in the proximal central parts of the Gulf of Cadiz and to $\sim$15 km in the most distal central parts [*González et al.*, 1996, 1998; *Gràcia et al.*, 2003; *Gutscher et al.*, 2002; *Zitellini et al.*, 2001]. The Iberian mainland represented by the Variscan Iberian Massif shows a crustal thickness of approximately 30 km [*Carbonell et al.*, 2003; *Fernàndez et al.*, 2004; *González et al.*, 1998; *ILIHA DSS Group*, 1993]. Three-dimensional modeling integrating gravity, elevation, heat flow and seismic data reveals that the Moho in the Alboran region shallows from maximum values of 34–36 km beneath the central Betics and Rif to 18 km beneath the western Alboran Basin and less than 14 km in eastern Alboran Basin [*Torné et al.*, 2000]. Values concerning the depth of the lithosphere-asthenosphere boundary are scarcer. According to *Torné et al.* [2000], the lithosphere thins dramatically from the Betic-Gibraltar-Rif belt (140–150 km) toward the central and eastern parts of the Alboran Basin (<50 km). This pattern is in agreement with seismic tomography studies, which show strong lateral variations in *P* wave velocity [e.g., *Blanco and Spakman*, 1993; *Calvert et al.*, 2000; *Gutscher et al.*, 2002; *Seber et al.*, 1996b]. These studies also show that low velocities in the depth range of 60–150 km are not restricted to the Alboran Basin but extend to the African mainland beneath the Atlas Mountains. A recent integrated study across the SW Iberian margin shows that the lithospheric thickness attains values of 115–125 km in the eastern Atlantic beneath the easternmost Horseshoe Abyssal Plane and the northeastern Seyne Abyssal Plane in agreement with the age of the oceanic lithosphere in this region [*Fernàndez et al.*, 2004]. Beneath the SW Variscan Iberian Massif, the same study proposes either a thinning of the lithosphere by 20–25 km or a reduction of the mantle density by $\sim$25 kg m^{-3} at lower lithospheric levels due to depletion during the Hercynian orogeny.

[12] There are several hypotheses about the evolution of this region. While some authors speak up for extensional collapse of a thickened crust to explain the Alboran Basin and westward migration of the Gibraltar arc [*Dewey*, 1988; *Doblas and Oyarzun*, 1989; *Platt and Vissers*, 1989], others invoke delamination as the leading subcrustal process [*Calvert et al.*, 2000; *Docherty and Banda*, 1995; *Seber et al.*, 1996b] on the basis of seismic reflection and tomography data. Finally, *Gutscher et al.* [2002] interpret seismic reflection and tomography data of the Gulf of Cadiz as evidences of active east dipping subduction as do also *Royden* [1993] and *Lonergan and White* [1997]. On the other side, southward [*Morales et al.*, 1999; *Sanz de Galdeano*, 1990], northward [*Torres-Roldan et al.*, 1986] and westward [*Zeck*, 1997] subduction affecting the Alboran region have also been invoked to explain geological and geophysical evidences. These disparities also exist for the nature of the crust in the Gulf of Cadiz. According to several authors [*González et al.*, 1996, 1998; *Dañobeitia et al.*, 1999; *Gràcia et al.*, 2003; *Tortella et al.*, 1997] the Gulf of Cadiz region is floored by the continental Hercynian crust, the transition to the oceanic domain being located further to the west, near the deep abyssal planes [e.g., *Purdy*, 1975; *Sartori et al.*, 1994; *Malod et al.*, 2003]. Other authors propose that during the opening of the Atlantic Ocean and the drifting of Africa relative to Iberia a narrow corridor of oceanic crust formed between both plates [e.g., *Flinch et al.*, 1996; *Maldonado et al.*, 1999] and that this corridor would still persist beneath the Gulf of Cadiz [*Gutscher et al.*, 2002].

2.2. Atlas-Sahara Domain

[13] The E-W trending High Atlas and its northern, NE-SW trending branch, known as the Middle Atlas, are the result of the Mesozoic rifting affecting the central north Atlantic and the western Tethys and the subsequent Cenozoic collision involving Africa and Europe [e.g., *Piqué et al.*, 1987; *Jacobshagen et al.*, 1988]. Although the Paleozoic basement crops out locally in antiformal culminations, the Middle and High Atlas consist mostly of slightly deformed Mesozoic rocks that once filled the most prominent Triassic and Jurassic troughs generated after extension and rifting. [*Beauchamp*, 1988; *Laville and Petit*, 1984; *Arboleya et al.*, 2004]. Rifting lasted to the end of the Liassic when the initiation of regional subsidence dominated during the middle and the end of the Mesozoic [*Gómez et al.*, 1998]. The stress field between Europe and North Africa changed to compression at the very end of the Mesozoic. Evidence of growth folding affecting latest Cretaceous sediments [*Froitzheim et al.*, 1988; *Herbig*, 1988; *Charroud*, 1990] marks the initiation of the Alpine orogeny in Northern Africa. Fault reactivation together with the development of new structures led to important tectonic inversion [*Beauchamp et al.*, 1996]. Deformation in the Middle and High Atlas indicates upper crustal conditions with weak or no metamorphism [*Teixell et al.*, 2003; *Arboleya et al.*, 2004]. Compressional deformation, evidenced by tectonic inversion of normal faults, is heterogeneously distributed: narrow basement-involving deformation bands [*Frizon de Lamotte et al.*, 2000] are

separated by broad synclines and tabular plateaus. Evaluation of the shortening due to Alpine compression yields values of 10% to 20% [*Brede et al.*, 1992], around 10%–15% [*Zouine*, 1993], up to 25% [*Beauchamp et al.*, 1999] and between 17% and 24% [*Teixell et al.*, 2003] in the High Atlas and around 5 km in the Middle Atlas [*Gómez et al.*, 1998; *Arboleya et al.*, 2004].

[14] Alkaline Paleogene to Quaternary volcanism has been identified in the Middle Atlas. The age of this volcanism has been dated by *Harmand and Cantagrel* [1984] as going from the Eocene (35 Ma) to the Miocene (15 to 6 Ma) and to the Quaternary (1.8–0.5 Ma) showing a relation between the age and the different provinces: Older volcanism is found in the northern and southern borders of the High Atlas whereas more recent events appear to the north, in the Middle Atlas. The tectonic context in which this volcanism appears is not yet fully understood and was explained by *Harmand and Moukadiri* [1986] as the result of upper mantle deformation which permitted partial melting in a compressive regime.

[15] In spite of the interest of the area, no vertical incidence seismic data has been acquired in the Middle and High Atlas and little seismic refraction information is available. *Tadili et al.* [1986] have modeled refraction and wide-angle data from an experiment in 1975 and concluded that crustal thickness varies from 25 km along the Atlantic coast of Morocco to 40 km near Imilchil in the central High Atlas. Other values of crustal thickness are 38 km from Midelt and 35 km around Er-Rachidia, all located in the Central High Atlas (see Figure 1 for location). Part of the same data has been interpreted by *Makris et al.* [1985], who conclude that the crustal thickness of the western High Atlas, the most elevated part of the orogen, ranges from 34 to 38 km, depending on the assumed thickness of the sedimentary cover. In addition, they find a very low velocity zone at 60–80 km depth underneath the western coast of Morocco. Another seismic refraction experiment was carried out further to the east in 1986 [*Wigger et al.*, 1992]. The resulting models show that the crust is thickest underneath the northern border of the High Atlas near Midelt, reaching 38–39 km, thinning to the south and to the north to 35 km. Also in these data, a low velocity zone in the uppermost mantle (below 40–45 km) underneath the transition from the High to the Middle Atlas is interpreted to be related to the influence of a hot mantle in a relatively high position. A coincident magnetotelluric survey gives a high-conductivity zone in the crust, dipping from the surface in the southern border of the High Atlas (Er-Rachidia) to the middle or lower crust below the Middle Atlas [*Schwarz et al.*, 1992]. Additional information about the crustal thickness has been recently obtained by receiver function studies. The results show that the Moho underneath Midelt is located between 36 km [*Sandvol et al.*, 1998] and 39 km [*van der Meijde et al.*, 2003].

[16] Geophysical models as well as estimations of tectonic shortening show that the high topography of the Atlas is not supported by the crust alone [*Teixell et al.*, 2003]. In fact, gravity modeling by *Seber et al.* [2001] suggests that the crust underneath the High Atlas is about 5 km thinner than expected by topography compensated at the Moho. The hot, low velocity mantle underneath the Atlas seen in tomography models may thus help to support the topography [*Seber et al.*, 1996b]. Scarce heat flow data yield values of 54 mWm^{-2} in the High Atlas and up to 85 mWm^{-2} in the Middle Atlas [*Rimi*, 1999]. On the basis of temperature-Vp dependence, Rimi concludes that the temperature in the crust-mantle boundary in the Middle Atlas is 890°C decreasing to around 695°C in the transition Middle-High Atlas and to 511°C in the High Atlas.

3. Method

[17] The numerical model is based on the joint interpretation of thermal and mass distribution related data. The temperature distribution in the lithosphere is often interpreted by using the surface heat flow and additional information such as lithospheric thickness from surface wave or *S* wave tomography. Since the relationship between seismic velocities and temperatures is not well known and may depend strongly on the presence of fluids in the mantle, we prefer to base our model on the relation between temperatures and densities, defined by the thermal expansion coefficient α. Increasing temperature results in decreasing density through the following relation:

$$\rho(T) = \rho_0 * [1 - \alpha(T - T_0)],$$

where $\rho(T)$ is the density at a given temperature T (°C), ρ_0 (kg/m^3) is the density at temperature T_0 (usually ambient temperature), and α is the thermal expansion coefficient (K^{-1}).

[18] Therefore, increasing the mantle temperature results in decreasing the average mantle density. These variations in mantle density together with those associated with lateral crustal thickness/lithological variations influence several measurable fields: gravity anomalies, geoid height and topography.

[19] Other effects that may potentially influence the density distribution in the mantle are pressure and phase changes. The influence of the compaction can be neglected, since lateral pressure variations are less than 1% and the corresponding density variations are therefore very small. The main phase transition within the model domain is the transition from spinel to garnet peridotite. This phase transition is often supposed to induce density variations, however a recent exhaustive review of densities measured for different peridotites [*Lee*, 2003] shows that while the density depends strongly on the Mg-number (i.e., the depletion state), it does hardly change from the spinel to the garnet phase, not at all if one takes into account the error bars. Therefore the thermal expansion is considered to be the principal reason for lateral density variations in the mantle.

[20] We use a two-dimensional finite element (FE) algorithm to calculate the steady state temperature distribution

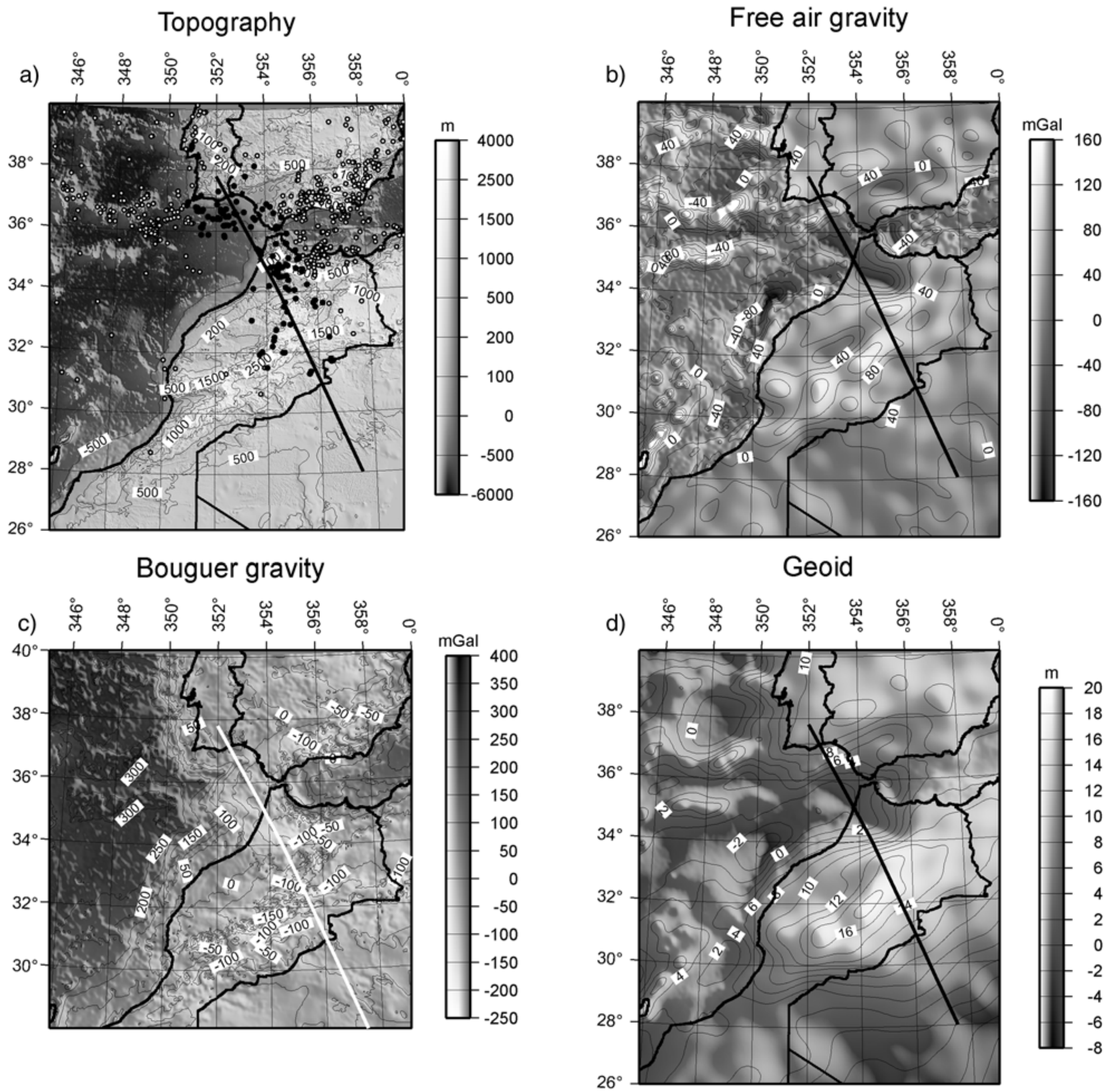

Figure 2. (a) Topography (ETOPO-2) and epicenters of earthquakes (all dots) from the CNSS Catalogue (1961–2001, $M > 3.5$). Black dots correspond to the earthquakes projected onto the profile in Figure 3. (b) Free-air gravity anomalies (TOPEX 1-min global data set). (c) Bouguer gravity anomalies [*Hildenbrand et al.*, 1988; *Mezcua et al.*, 1996]. (d) Geoid variations (EGM96). (e) Surface heat flow data [*Pollack et al.*, 1993; *Fernàndez et al.*, 1998; *Rimi*, 1999]. Thick black line in Figures 2a–2e represents the interpreted profile. See color version of this figure in the HTML.

with the following boundary conditions [*Zeyen and Fernàndez*, 1994]: constant surface temperature (15°C), no lateral heat flow at the vertical model boundaries, and a constant temperature of 1350°C at the base of the lithosphere The base of the lithosphere is modified interactively in order to find the best fitting model. The model space is subdivided into bodies corresponding to sediments, upper, middle, and lower continental crust, oceanic crust and lithospheric mantle. These bodies are characterized by their density, thermal conductivity and heat production. Once the temperature distribution has been determined, the densities are evaluated at each node of the FE grid and with this density distribution, the gravity, geoid, and topography anomalies are calculated.

[21] Topography is calculated under the assumption of local isostatic equilibrium with the compensation depth at

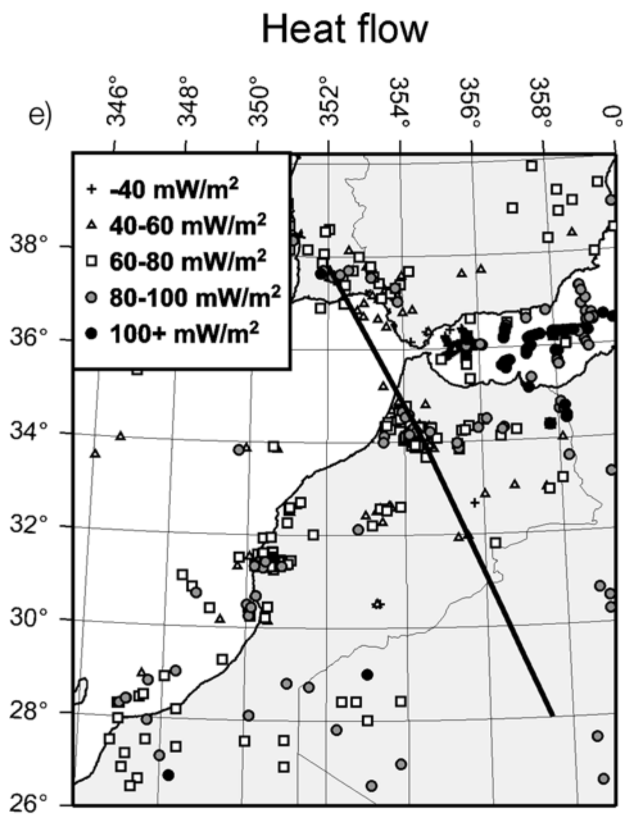

Figure 2. (continued)

the deepest point of the lithosphere within the model space. The obtained topography variations are calibrated with respect to average mid-oceanic ridge bathymetry [*Lachenbruch and Morgan*, 1990], resulting in the following formula applied to each column of the model:

$$h = \frac{\rho_a - \rho_L}{\rho_a} * H + h_0,$$

where

- h topography (m);
- ρ_a asthenospheric density (3200 kg/m^3);
- ρ_L average lithospheric density (kg/m^3);
- H thickness of the lithosphere (m);
- h_0 calibration constant (−2400 m).

If h becomes negative, one has to add the effect of water pressure:

$$h_- = \frac{\rho_a}{\rho_a - \rho_{water}} * h.$$

The gravity anomalies are calculated in two dimensions using the algorithm of *Talwani et al.* [1959]. For the calculation of the geoid, we convert the triangular elements of the grid into rectangular prisms with a large lateral extension in order to simulate two-dimensional anomalies and calculate the anomaly as (own development):

$$\Delta H = \frac{G\cdot\rho}{g}\left[xy\ln(z+R) + xz\ln(y+R) + yz\ln(x+R) - \frac{1}{2}\left[x^2 f(x,y) + y^2 f(y,x) + z^2 f(z,x)\right]\right]\Bigg|_{x_1-x_0}^{x_2-x_0}\Bigg|_{y_1-y_0}^{y_2-y_0}\Bigg|_{z_1-z_0}^{z_2-z_0}$$

where

$$f(a,b) = \arcsin\left(\frac{a^2+b^2+bR}{\sqrt{a^2+b^2}\cdot(b+R)}\right)$$

$$R = \sqrt{x^2+y^2+z^2};$$

- ΔH geoid anomaly (m);
- g gravimetric attraction at the Earth's surface (9.81 m/s^2);
- G universal gravity constant (6.67 $\times$ 10^{-11} m^{3}kg^{-1}s^{-2});
- x_1, x_2 x coordinates of the prism boundaries;
- y_1, y_2 y coordinates of the prism boundaries;
- z_1, z_2 z coordinates of the prism boundaries;
- (x_0, y_0, z_0) coordinates of the calculation point, all in meters;
- ρ density of the prism (kg/m^3).

4. Gravity, Heat Flow, Geoid, and Topography Data

[22] Most of the data have been obtained from publicly available worldwide databases and from local sources. Topography (Figure 2a) and free-air gravity (Figure 2b) are taken from the TOPEX global data sets (2-min grid spacing for topography, 1-min grid spacing for free-air gravity; ftp://topex.ucsd.edu/pub; [*Sandwell and Smith*, 1997]). Geoid height (Figure 2d) is taken from the EGM96 global model [*Lemoine et al.*, 1998]. Bouguer gravity data (Figure 2c) come from the Moroccan [*Hildenbrand et al.*, 1988] and Spanish [*Mezcua et al.*, 1996] gridded data sets. Offshore, the TOPEX 1-min global free-air data set has been reduced to Bouguer anomalies using the ETOPO-2 bathymetries. Heat flow data (Figure 2e) come from *Pollack et al.* [1993], *Fernàndez et al.* [1998] and *Rimi* [1999]. In Figure 2a, we have also included epicenters of the earthquakes with magnitude *M* > 3.5 that happened in the region between 1961 and 2001 taken from the CNSS Catalogue (available at http://quake.geo.berkeley.edu/cnss/catalog-search.html). In order to avoid effects of sublithospheric density variations on the geoid, we have removed the geoid signature corresponding to the spherical harmonics developed until degree and order 8 [*Bowin*, 1991].

[23] The heat flow values were projected from a 100 km wide stripe on both sides of the profile. In the northern Gulf

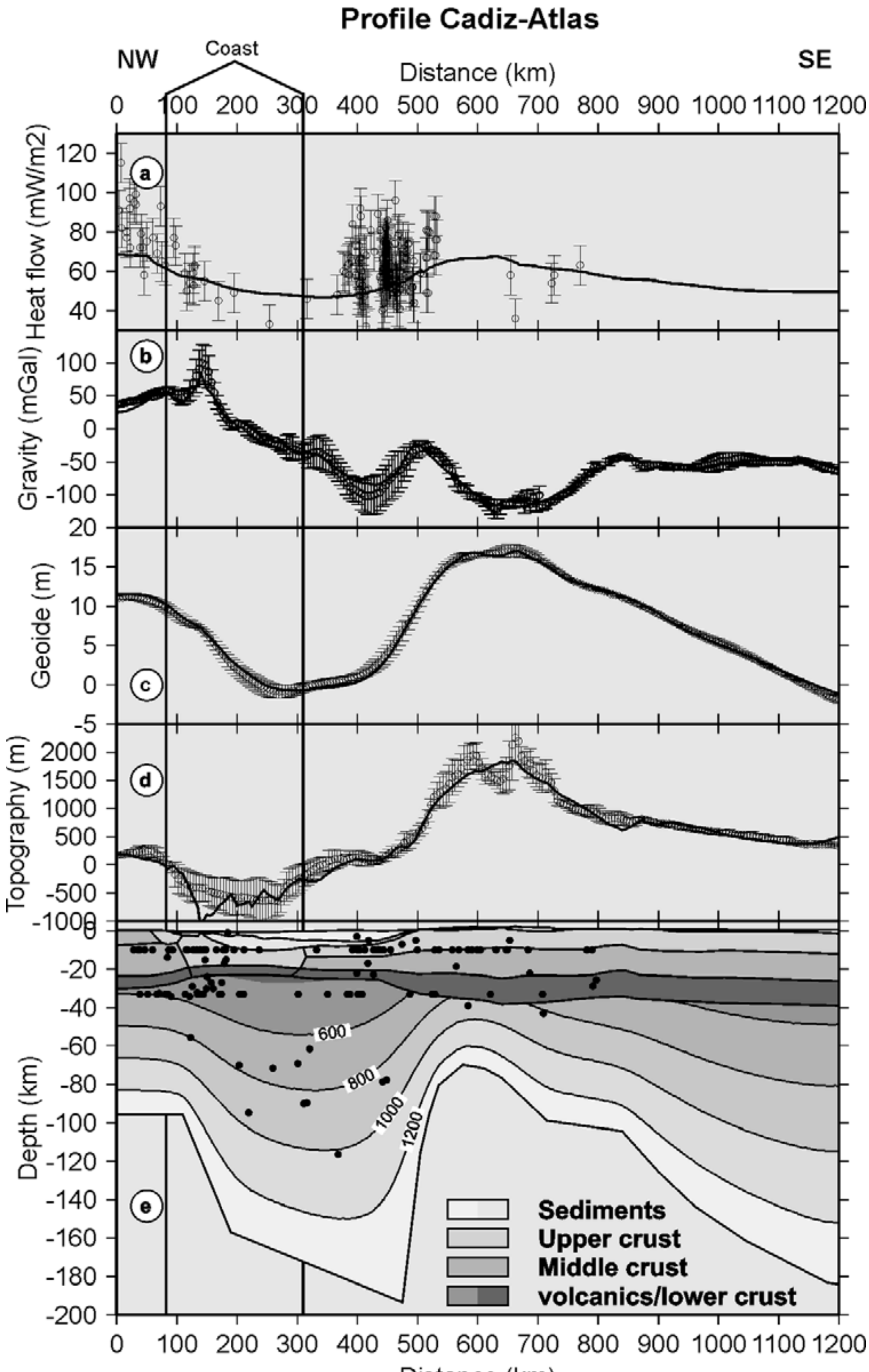

Figure 3. Modeling results. The top four graphs (Figures 3a–3d) show data and effects of the model. The data are represented by dots with error bars, corresponding to the estimated data uncertainty (surface heat flow, Figure 3a) or to the standard deviation within a range of 50 km to each side of the profile (Bouguer gravity, geoid and topography, Figures 3b–3d). The model effect is shown by the continuous lines. Figure 3e shows the model with a vertical exaggeration of 3.2. The dots mark earthquake hypocenters projected onto the model from a stripe of 100 km width each side of the model.

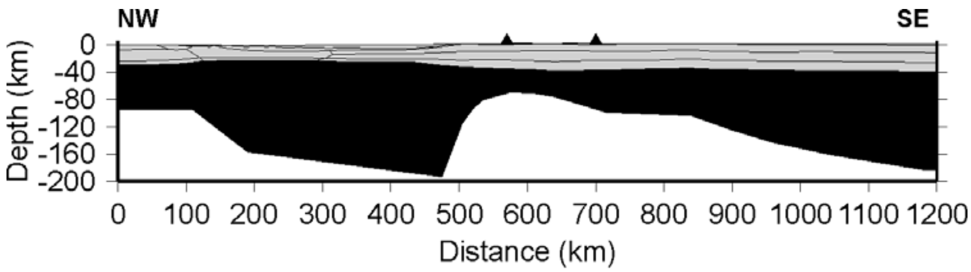

Figure 4. Model at scale 1:1 showing the modeled real slope of the topography of the lithosphere-asthenosphere boundary. Gray, crust; black, lithospheric mantle. Triangles at the surface near km 600 and km 700 mark Neogene volcanic activities.

of Cadiz and the Gharb Basin, the data present a wide scatter, mainly due to groundwater flow and hydrothermal activity, with average values of approximately 70 mW/m^2. In the central and southern Gulf of Cadiz, low heat flow prevails (40–50 mW/m^2) probably related to thrust stacking and rapid sedimentation. In the High Atlas and its southern slope, the few measured heat flow values cluster around 60 mW/m^2.

[24] The gravity, geoid, and topography data were averaged every 5 km from a 50 km wide stripe on both sides of the profile. Pronounced maxima for free-air gravity, geoid, and topography are located all along the Atlas Mountains with a strong correlation between each other. This good correlation is an indicator for a topographic compensation at relatively large depth, since otherwise the free-air gravity anomalies would tend toward zero. The usually expected anticorrelation between Bouguer anomalies and topography is only partly present. It is, for example, interesting to compare the Atlas with the Rif Mountains in northern Morocco which have a similar Bouguer minimum but much lower topography. Also the gravity data along the profile (Figure 3b) show that the Bouguer anomalies in the Atlas Mountains are not very pronounced with respect to the bordering lowlands to the north and to the south, in contrast to the free-air anomalies.

5. Modeling Results

[25] The first qualitative analysis of the data in the preceding section indicated already a probable influence of the deep lithosphere on the state of isostatic equilibrium. In particular, the combination of large negative Bouguer and geoid height anomalies observed in the Gulf of Cadiz region, indicates an overcompensated crustal isostasy where a deep lithospheric root is required to compensate the shallow density deficit related to the water layer and the thick sediment accumulation. In contrast, the observed gravity and geoid fields in the Atlas Mountains suggest an undercompensated crustal isostasy with a very thin lithospheric mantle beneath a mountain range whose crustal thickening is much less than that required to produce the observed topography.

[26] The results of quantitative modeling are presented in Figures 3 and 4. Different crustal bodies have been considered according to their densities, thermal conductivity and volumetric heat production (see Table 1). The crustal structure in the Variscan Iberian Massif (NW end of the profile) has been slightly modified from *Fernàndez et al.* [2004] to simulate the presence of the high density and high heat production Pyrite Belt and Accretionary Complex running parallel to the profile in this area. The section corresponding to the Gulf of Cadiz has been constrained by seismic reflection and wide-angle refraction data summarized in *Gràcia et al.* [2003] and *González et al.* [1998]. Whether the crust beneath the thrusted sedimentary units belongs to the South Iberian margin or to the North African margin is quite uncertain and therefore we have considered a "transition" crust with average properties in the upper and middle crust. In the Gharb Basin, the profile runs parallel to the External Rif Front and we have used geological cross sections by *Platt et al.* [2003] to estimate the average depth to basement. Crustal thickness values beneath the High Atlas and the Sahara Platform have been constrained by seismic refraction [*Wigger et al.*, 1992] and receiver function analyses [*Sandvol et al.*, 1998; *van der Meijde et al.*, 2003]. Along the African section, we have considered three main crustal layers with similar petrophysical properties as

Table 1. Properties of the Different Bodies[a]

N	Density, kg/m^3	Heat Production, μW/m^3	K, W/(K $\times$ m)
1	2000	1.2	2
2	2400	1.2	2.3
3	2600	1.2	2.4
4	2650	1.2	2.4
5	2300	1.2	2.1
6	2800	1.0	2.0
7	2800	2.5	3.5
8	2740	2.0	3.0
9	2750	1.2	2.5
10	2730	1.5	2.5
11	2800	0.6	2.4
12	2800	0.6	2.4
13	2950	0.2	2.1
14	2950	0.2	2.1
15	2950	0.2	2.1
16	3200	0.02	3.2

[a]Numbers (N) correspond to those of Figure 5. K is the thermal conductivity. The density ρ in the mantle (body 16) is temperature dependent. The given density corresponds to the one at 1350°C and $\rho(T) = \rho_0[1 - 3.5 \times 10^{-5}(T-1350°C)]$.

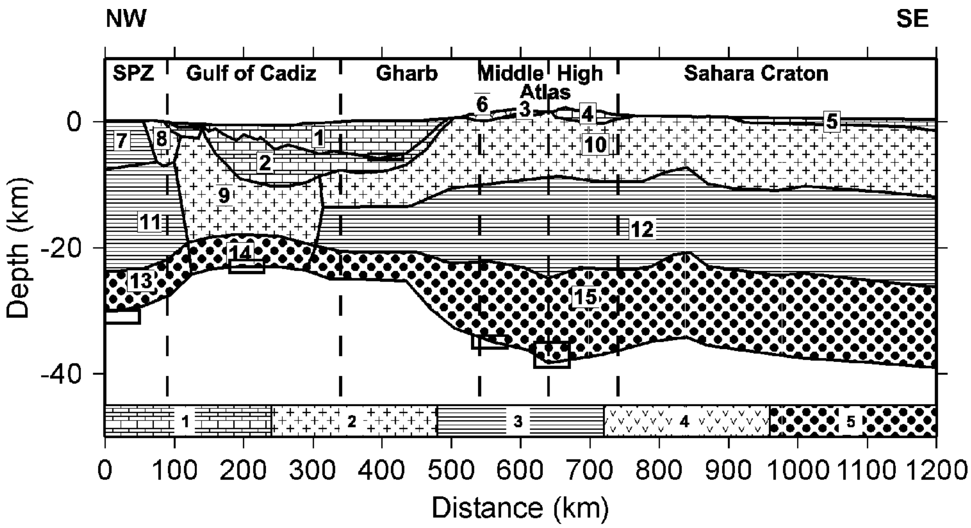

Figure 5. Blowup of the crustal structure (9× vertical exaggeration). The different rectangles represent seismic a priori information for crustal and sedimentary thicknesses. The numbers within the different bodies refer to those in the first column of Table 1. Shadings and corresponding densities [kg/m^3] are as follows: 1, sediments (2000–2650); 2, upper crust (2730–2750); 3, middle crust (2800); 4, volcanic rocks (2800); 5, lower crust (2950). See color version of this figure in the HTML.

in the Variscan Iberian Massif (Table 1). The limits between upper, middle, and lower crust correspond approximately to the seismic velocities of 6.3 and 6.6 km/s given by *Wigger et al.* [1992]. Finally, at shallow levels, we have defined a volcanic "body" in the Middle Atlas corresponding to Plio-Quaternary basalts (cones in Figure 4) as well as some Mesozoic and Neogene basins in the High Atlas and on the Sahara Platform.

[27] Figure 3 shows the observed and calculated values of surface heat flow, Bouguer anomaly, geoid height, and elevation for our preferred model. For the geoid anomalies, the mean slope of the calculated data has been adjusted to the one of the measured data in order to remove the very long wavelengths having sources below the lithosphere. The resulting crustal and lithospheric structure is shown in the lower panel with a vertical exaggeration of 3 and in Figure 4 without vertical exaggeration. The model results are in good agreement with the data observed with the exception of some local misfits. Short wavelength misfits between the observed and calculated elevation and Bouguer anomaly are found along the Gulf of Cadiz and the Atlas Mountains (Figures 3b and 3d), which are attributed to local features that are out of the scope of our regional modeling, e.g., related to the gross geometry adopted for the sediments and/or the top of the basement. The major misfit in Bouguer anomaly (<20 mGal) is in the NW end of the profile and is probably related to three-dimensional effects since the profile runs perpendicular to a steep horizontal gradient. Elevation shows also a large misfit (~1000 m) in the northern Gulf of Cadiz related to the basement high of the Guadalquivir Bank possibly supported by flexural lithospheric rigidity (see discussion). The geoid anomaly is fitted very well. The surface heat flow follows the observed general trend, but the large spread in the measurements makes it more difficult to evaluate the quality of the match.

[28] The most outstanding feature related to the lithospheric structure (Figures 3e and 4) is the important topography of the base of the lithosphere (1350°C isotherm). The lithospheric thickness varies from about 90 km under the Variscan Iberian Massif in agreement with earlier modeling results [*Fernàndez et al.*, 2004], to 160–190 km underneath the Gulf of Cadiz and Gharb Basin, decreasing strongly to 70 km underneath the Middle Atlas and thickening gradually toward the Sahara Platform to 180 km or more. Taking other temperatures for the limit between lithosphere and asthenosphere (temperatures between 1250° and 1400°C have been proposed in the literature) would change these values by not more than ±10 km. Strong lithospheric thickening beneath the Gibraltar arc is also imaged by seismic tomography [e.g., *Calvert et al.*, 2000; *Seber et al.*, 1996a] and combined thermal and gravity modeling [*Torné et al.*, 2000]. Hypocenter localizations along the profile seem to corroborate this interpretation. Projection of the hypocenters of earthquakes recorded between 1961 and 2001 in a range of 150 km around the profile (Figure 3e) show that, with one exception, the deepest earthquakes follow well the isotherm of 900° ± 50°C that would correspond to the base of the mechanical lithosphere. Negative velocity anomalies in the range of 2–3% are found beneath the Middle-High Atlas coinciding with a large volcanic zone, thus supporting a lithospheric thinning in this region.

[29] Figure 5 shows a blowup of the final crustal structure along the modeled profile and the constraints used to define the preliminary crustal model. The crust thins from about 30 km beneath the Variscan Iberian Massif to less than 23 km in the central part of the Gulf of Cadiz. Crustal

thickness is maintained around 25 km almost until the External Rif front from where it increases up to maximum values of 38 km beneath the northern border of the High Atlas. Further to the SE the crustal thickness attains values of 35 km under the Anti-Atlas from where it increases steadily toward de Sahara Platform until 39 km in the southeastern end of the model profile (Tindouf Basin). A remarkable feature in the crustal structure is the large sediment accumulation affecting the Gulf of Cadiz and the Gharb Basin, where the thickness of Neogene and Quaternary sediments increases from a few hundred meters in the northern margin of the Gulf of Cadiz to more than 5.5 km in the Gharb Basin [*Litto et al.*, 2001]. The top of the basement that is overlain by thrusted and stacked sediments of different age, reaches depths of 10 km and 8 km below the Gulf of Cadiz and Gharb Basin, respectively. These values, however, must be considered with some caution since our profile runs obliquely to the main tectonic structures and therefore lateral structures could modify the obtained geometries.

6. Discussion

[30] The modeling approach used in the present study integrates different observables (topography, Bouguer anomaly, geoid height, and surface heat flow), which are governed by the temperature and density distribution in the crust and lithospheric mantle and partly constrained by available seismic and geological data. Basic assumptions of the model are as follows: (1) the density of the asthenosphere is constant everywhere; (2) the lithosphere does not support vertical shear stresses, i.e., the topography is entirely supported by local isostasy; and (3) the lithosphere is in thermal steady state. These assumptions impose some limitations in interpreting the resulting lithospheric structure that will be discussed in detail in this section.

[31] The most outstanding result obtained from the present study is the large variation of the depth of the lithosphere-asthenosphere boundary along the model profile. This variation is mainly constrained by geoid and topography data since both data sets are sensitive to density variations at deep levels. In contrast, surface heat flow and gravity data are not able to image reasonably well the lithospheric structure. Figure 6 illustrates how sensitive are the different observables to the topography of the base of the lithosphere. In Figure 6, we present a model with a flat lithosphere-asthenosphere boundary at 110 km depth. The density distribution within the crust and the form of the different crustal interfaces have been slightly modified in order to keep the gravity anomalies within the range of measured values. With such a model, the amplitude of the geoid anomalies becomes too large, whereas the topography is very badly explained mainly in the Gulf of Cadiz/Gharb area and in the Middle Atlas.

[32] This shows that topography and geoid heights are far from being compensated at Moho level and that strong variations in the lithosphere-asthenosphere boundary are required to fit all the observables. It can be argued that active flow in the sublithospheric mantle related to either sinking slabs or mantle plumes can modify the density of the asthenosphere by a small percentage and consequently the derived lithospheric thickness. Certainly, geoid height variations are sensitive to density heterogeneities far beneath the lithosphere-asthenosphere boundary and this is the primary reason for filtering the large wavelength components of the measured geoid. Concerning to topography, it is expected that at temperatures above those corresponding to the lithosphere-asthenosphere boundary, rocks are not able to support noticeable static vertical forces, and therefore taking the effective level of compensation at the base of the lithosphere is a good approach [*Sobolev et al.*, 1996].

[33] A critical assumption for our modeling is that of local isostasy. The response of the lithosphere to loading depends on its rigidity, and the amplitude and wavelength of the loads. For large wavelengths (>100 km), the lithosphere is not able to support vertical shear stresses and then isostatic equilibrium is produced under local isostasy [*McKenzie and Bowin*, 1976]. However, for short wavelengths part of the load can be supported elastically resulting in a smoother lithospheric deflection. We have carried out an analysis to calculate which part of the topography may be supported by an elastic plate. For that, we filtered the topographic data in the Fourier domain with the following coefficients [*Turcotte and Schubert*, 1982, p. 123]:

$$\Omega(k) = \frac{g \cdot \rho_{topo}}{D \cdot k^4 + g \cdot \left(\rho_a - \rho_{topo}\right)} H(k),$$

where Ω and H are the Fourier coefficients of the plate deformation and the topography respectively, k the wave number, D the flexural rigidity, g the gravitational acceleration and ρ_{topo} and ρ_a the densities of topography (taken here as average crustal density of 2800 kg/m^3) and the asthenosphere, respectively. The resulting deformation is then retransformed into the corresponding topography in local isostatic equilibrium by multiplication with the factor $(\rho_a - \rho_{topo})/\rho_a$ and compared with the measured topography. Figure 7 shows the results of this calculation. The thin dashed line corresponds to the measured topography, the thin continuous line to the modeled one (Figure 3). Since the effect of an elastic plate is first of all to smoothen the topography, we carried out the calculations in different ways left and right of 450 km (vertical line): Left of 450 km, the rough topography corresponds to the modeled one, so we are interested to see whether an elastic plate could support part of the stresses due to internal density variations. Right of this position, the calculation was done with the rough measured topography in order to see how much of it may be supported elastically.

[34] The thick continuous line represents the topography filtered by a 10 km thick elastic plate. Left of 450 km, this line fits the observed topography to better than 300 m, indicating that the difference between calculated and measured topography may well be supported by such a plate. A 30 km thick plate that takes into account the colder lithosphere would result in a maximum difference of less than 100 m in the Gulf of Cadiz (dashed line). Right of 450 km, the calculated topography in the Atlas mountains

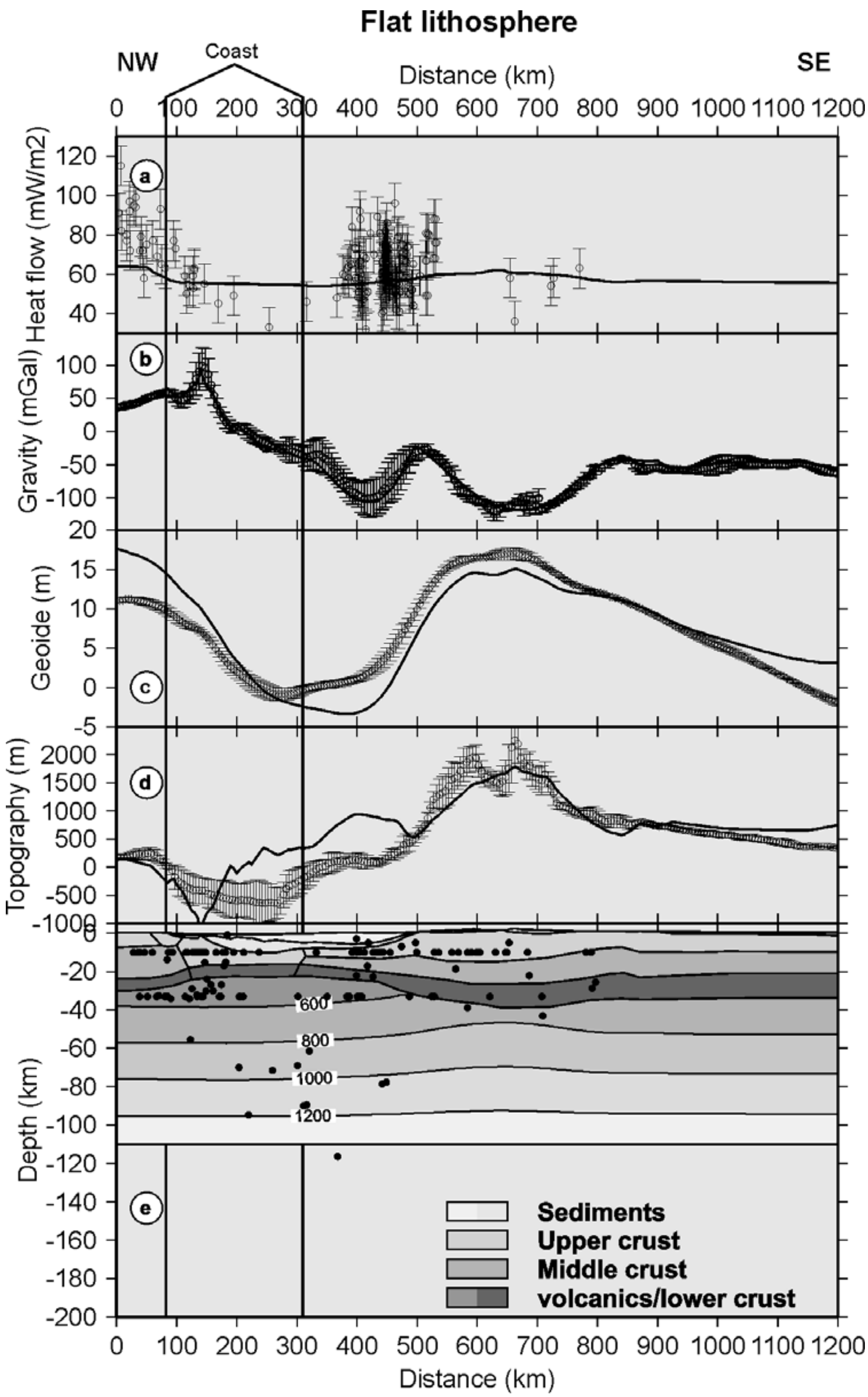

Figure 6. Model with a flat base of the lithosphere showing the influence of the temperature variations in the uppermost mantle on the geoid and the topography.

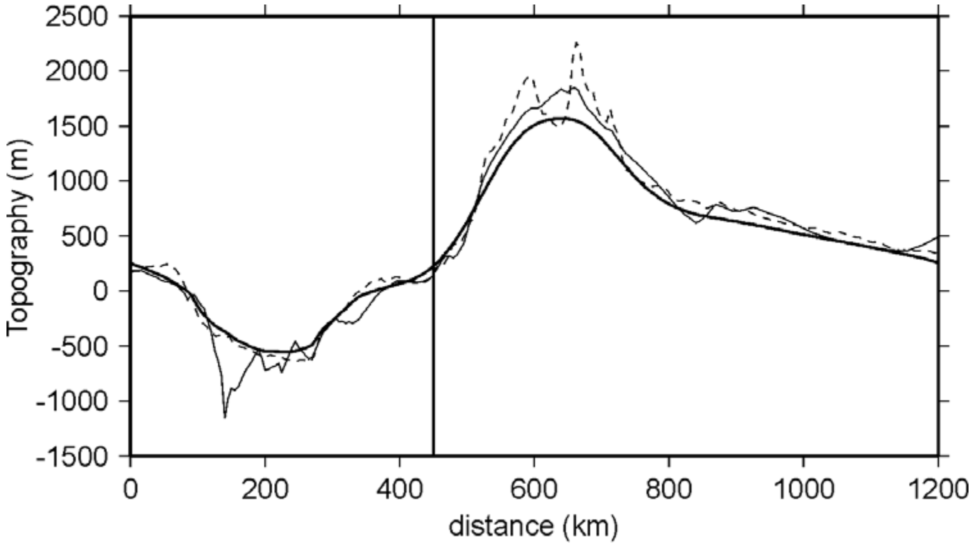

Figure 7. Elastic support by an elastic plate. The thin continuous line represents the topography calculated with our model in local isostatic equilibrium (Figure 3d); the thin dashed line represents the measured topography. The thick continuous line corresponds to the topography expected for a 10 km thick elastic plate. The vertical line at 450 km separates two areas treated differently (see text).

is up to 250m higher i.e., less filtered than the one supported by a 10 km thick elastic plate. However, due to the high temperatures, 10 km are probably strongly overestimated. A 5 km thick plate would result in a topography to within 150m of the calculated one.

[35] The temperature distribution within the lithosphere has been calculated under the assumption of thermal steady state. This assumption is particularly valid in old tectonothermal provinces as the Variscan Iberian Massif and Moroccan Meseta as well as the Sahara Platform. However, the Gulf of Cadiz region and the Atlas Mountains underwent major tectonothermal events during the Cenozoic producing transient perturbations in the temperature distribution. On the one hand, quantifying these perturbations requires a much better knowledge of the geodynamic evolution of these regions than is presently available. On the other hand, our model accounts for a lithospheric density-depth distribution that is compatible with elevation, gravity, and geoid observations independent of the actual temperature distribution. Thus the calculated temperature distribution within the lithosphere as well as the depth of the lithosphere-asthenosphere boundary must be interpreted as average physical conditions necessary to produce the required density distribution rather than actual thermal boundaries. Steady state thermal modeling tends to underestimate/overestimate the actual lithospheric thickness when the modeled thickening/thinning processes are still under transient conditions. In consequence, the imaged lithospheric thickness beneath the Gulf of Cadiz and the Rif could even exceed 200 km whereas beneath the Atlas Mountains the calculated lithospheric thinning could be more conspicuous.

[36] The calculated lithospheric thickness beneath the Middle and High Atlas is quite sensitive to the considered crustal thickness and density. Assuming a maximum crustal thickness of 39 km in this region we obtain a lithospheric thickness of approximately 90 km indicating that, in this case, the lithosphere would not be thinned strongly with respect to a typical Hercynian one (approximately 100 km). However, most seismic data, the very little Alpine deformation and the small sedimentation observed in geological cross sections [*Teixell et al.*, 2003; *Arboleya et al.*, 2004] suggest that the crust must be thinner, probably as thin as 35–36 km in the Middle Atlas, though locally, it might reach 38–39 km in the northern border of the High Atlas [*van der Meijde et al.*, 2003; *Ayarza et al.*, 2005].

[37] Lateral variations in lithospheric thickness are also evidenced by seismic tomography data, showing a high-velocity body ($\Delta Vp \sim 2-4$ %) beneath most of the western Betics and Rif that strikes NE-SW, dips roughly SE, and extends over a depth range between 60 and 350 km [*Bijwaard and Spakman*, 2000; *Calvert et al.*, 2000]. At higher depths, the velocity perturbation becomes more diffuse but can be followed down to 650 km. Tomography studies also show the existence of low velocity zones extending from the surface to 150 km depth beneath the Atlas and the Alboran Basin [*Bijwaard and Spakman*, 2000; *Calvert et al.*, 2000]. Refraction data modeled by *Wigger et al.* [1992] show a low velocity zone right north of Midelt, between 40–50 km depth and *Makris et al.* [1985] find another low velocity zone in the transition from the western High Atlas and the Moroccan coast at a depth of 60–80 km.

[38] Another argument favoring a prominent lithospheric thickening in the region is the occurrence of intermediate seismicity distributed over the western Betics-Alboran-Rif area and also over the northern half of the Gulf of Cadiz region [e.g., *Calvert et al.*, 2000; *Mezcua and Rueda*, 1997] (see also Figures 2a and 3e). Further evidences for litho-

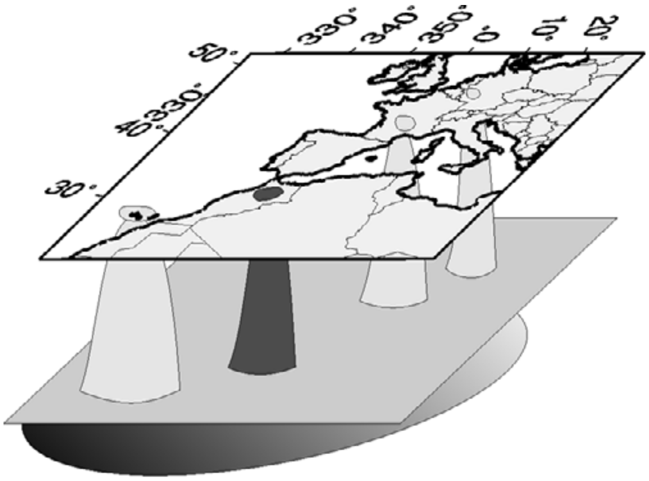

Figure 8. Sketch of the distribution of plumes in western Europe and northwestern Africa acting as "escape valves" for a large reservoir of hot material in the deep upper or uppermost lower mantle. The light shaded plumes show well-established zones of upwelling hot material with the corresponding volcanic areas at the surface (from the SW, Canary Islands, French Massif Central, and German Eifel). The dark shaded plume represents the hypothetical plume underneath the Atlas Mountains. See color version of this figure in the HTML.

spheric mantle thinning underneath the Middle Atlas come from alkaline Plio-Quaternary volcanism [*Hammond and Humphreys*, 2000a, 2000b].

[39] Much attention has been paid in interpreting the lithospheric thickening beneath the Gibraltar Arc and the adjacent thinning in the Alboran Basin, which gave rise to the formulation of several geodynamic models related to convective removal and orogenic collapse [*Dewey*, 1988; *Doblas and Oyarzun*, 1989; *Platt and Vissers*, 1989], mantle delamination [*Calvert et al.*, 2000; *Docherty and Banda*, 1995; *Seber et al.*, 1996b], and subduction [*Gutscher et al.*, 2002; *Lonergan and White*, 1997; *Morales et al.*, 1999; *Royden*, 1993; *Sanz de Galdeano*, 1990; *Torres-Roldan et al.*, 1986; *Zeck*, 1997]. Our results show that this peculiar topography of the lithosphere-asthenosphere boundary is not restricted to the Gibraltar Arc-Alboran Basin but extends obliquely to the southwestern outer regions, where thickening affects the Gulf of Cadiz and the Gharb Basin and thinning affects the western High Atlas and the Middle Atlas. Thereby, the lithosphere-asthenosphere boundary draws a lithospheric slab striking SW-NE in agreement with that proposed by *Calvert et al.* [2000]. However, in our case this slab would then extend from the western Betics to at least the Gharb Basin posing questions on the Alboran-generating mantle delamination hypothesis. On the other hand, we do not have evidences of oceanic crust flooring the Gulf of Cadiz. Rather, our model supports a continental character of the crust continuously from the Iberian to the African margin, which would rule out the hypothesis of an east directed active subduction in the Gibraltar Arc in its position proposed by *Gutscher et al.* [2002]. The position of the active margin, if it exists, should be further away from the Gibraltar arc, west of our profile.

[40] Geological and geophysical data (Neogene volcanism, heat flow, elevation, geoid height, and tomography) indicate that the modeled mantle thinning could extend along the western High Atlas and the Middle Atlas. One hypothesis is to relate this thinning to the above mentioned lithospheric thickening as a side effect of a retreating slab or a sinking detached body, which would trigger active flow in the less viscous asthenosphere. An alternative explanation is to dissociate these processes and to assume a small plume-like asthenospheric upwelling.

[41] Thinning of the lithospheric mantle simultaneous with crustal thickening or no crustal stretching can occur by thermal erosion produced by a mantle plume. The activity of such a plume could have started during the Eocene coinciding with alkaline volcanism reported in the High Atlas [*Harmand and Cantagrel*, 1984]. According to *d'Acremont et al.* [2003], numerical modeling of mantle plumes indicates that the thermal erosion of a plume is concentrated above the plume head only in its initial stages, moving later to two large bordering zones. In this case, thermal erosion of the plume would presently concentrate along the Middle Atlas and/or the Anti-Atlas. Volcanism in the Middle Atlas is widespread along our profile. Access of magma to the surface might have been favored by the existence of a previously rifted and fractured crust. Our cross section does not cross any volcanic zone in the Anti-Atlas; however, Miocene to Quaternary alkaline volcanism has been described by *Berrahma et al.* [1993]. This plume could be considered as similar to those mapped under the French Massif Central [e.g., *Granet et al.*, 1995] or the Eifel in Germany [*Ritter et al.*, 2001]. Such a small plume may then be interpreted as one of several "escape valves" of a large hot reservoir deeper in the mantle postulated by *Hoernle et al.* [1995] (Figure 8).

[42] Farther SE of the Atlas Mountains, our model predicts a steady increase of the lithospheric thickness until values of around 180 km beneath the Sahara Platform toward the Precambrian terranes. Similar values are found from a global thermal study [*Artemieva and Mooney*, 2001] and a combined global geochemical and thermal analysis [*Poudjom-Djomani et al.*, 2001] in which the authors deduce that the lithospheric thickness for Proterozoic cratonic areas ranges between 140 and 200 km.

7. Conclusions

[43] We carried out a joint interpretation of surface heat flow, gravity, geoid, and topography data in order to investigate the thermal and density structure of the lithosphere along a profile crossing the Gulf of Cadiz and the Atlas Mountains near the towns of Meknes and Midelt. The crustal structure is based wherever possible on existing seismic data. The following principal conclusions can be drawn from the results:

[44] 1. The lithosphere underneath the Gulf of Cadiz is very thick in order to explain the observed bathymetry in the presence of a thick sediment pile and a thinned continental crust. The thickness of 160–190 km obtained in our model is significantly larger than should be expected for the area, surrounded by regions of about 100 km lithospheric thickness in Iberia and oceanic lithosphere with an age of 150 Ma in the Atlantic, corresponding typically to approximately 120 km thick lithosphere. The thickened region is interpreted as a lithospheric slab.

[45] 2. The Atlas Mountains cannot be supported isostatically only by a thickened crust. A thin (70 km), hot, low-density lithosphere is required to explain the high topography. This lithospheric thinning affects the northern border of the Central High Atlas and the Middle Atlas and could be related to a side effect of the lithospheric slab when it penetrates into the less viscous asthenosphere. Alternatively (and also our preferred interpretation), the lithospheric thinning can be related to a small mantle plume similar to those found in the French Massif Central [*Granet et al.*, 1995] and the Eifel in Germany [*Ritter et al.*, 2001], which form part of a hot and deep mantle reservoir system extending from the Canary Islands to central Europe [*Hoernle et al.*, 1995].

[46] 3. The lithosphere thickens steadily from the Atlas Mountains to the SE end of the model where a thickness of about 180 km has been obtained. These values are in good agreement with those proposed from global studies for Proterozoic regions.

[47] **Acknowledgments.** This work has been supported by the Spanish Ministerio de Ciencia y Tecnología through projects REN2001-3868-C03-02/MAR and BTE2000-0159 and the French-Moroccan Integrated Action 98/SDU/161. Scientific exchange and stays have been done in the framework of the NATO Collaborative Research Grant (EST.CLG.978922) and the European Science Foundation EUROCORES Programme on Euromargins (01-LEC-EMA22F). Two research visits of P. Ayarza to the University Paris-Sud have been funded by the University of Salamanca. We thank the two reviewers for constructive comments on a first version of the manuscript.

References

Arboleya, M. L., M. Charroud, A. Teixell, and M. Julivert (2004), A structural transect through the High and Middle Atlas of Morocco, *J. Afr. Earth Sci.*, *39*(3–5), 319–327, doi:10.1016/j.jafrearsci.2004.07.036.

Artemieva, I. M., and W. D. Mooney (2001), Thermal thickness and evolution of Precambrian lithosphere: A global study, *J. Geophys. Res.*, *106*, 16,387–16,414.

Ayarza, P., F. Alvarez-Lobato, A. Teixell, M. L. Arboleya, E. Tesón, M. Julivert, and M. Charroud (2005), Crustal structure under the central High Atlas mountains (Morocco) from geological and gravity data, *Tectonophysics*, in press.

Banda, E., J. Gallart, V. García-Dueñas, J. J. Dañobeitia, and J. Makris (1993), Lateral variation of the crust in the Iberian peninsula: New evidence from the Betic Cordillera, *Tectonophysics*, *221*, 53–66.

Banda, E., et al. (1995), Iberian Atlantic Margins Group investigates deep structure of ocean margins, *Eos Trans., AGU*, *76*, 25, 28–29.

Beauchamp, J. (1988), Triassic sedimentation and rifting in the High Atlas (Morocco), in *Triassic-Jurassic Rifting: Continental Breakup and the Origin of the Atlantic Ocean and Passive Margins*, edited by W. Mainspeizer, pp. 477–497, Elsevier, New York.

Beauchamp, W., M. Barazangui, A. Demnati, and M. El Alji (1996), Intracontinental rifting and inversion: Missour Basin and Atlas Mountains, Morocco, *AAPG Bull.*, *80*, 1459–1482.

Beauchamp, W., R. W. Allmendinger, M. Barazangi, A. Demnati, M. El Alji, and M. Dahmani (1999), Inversion tectonics and the evolution of the High Atlas Mountains, Morocco, based on a geological-geophysical transect, *Tectonics*, *18*, 163–184.

Berrahma, M., M. Delaloye, A. Faure-Muret, and H. E. N. Rachdi (1993), Premières données géochronologiques sur le volcanisme alcalin du Jbel Saghro, Anti-Atlas, Maroc, *J. Afr. Earth Sci.*, *17*, 333–341.

Bijwaard, H., and W. Spakman (2000), Non-linear global *P*-wave tomography by iterated linearized inversion, *Geophys. J. Int.*, *141*, 71–82.

Bijwaard, H., W. Spakman, and E. R. Engdahl (1998), Closing the gap between regional and global travel time tomography, *J. Geophys. Res.*, *103*, 30,055–30,078.

Blanco, M. J., and W. Spakman (1993), The *P*-wave velocity structure of the mantle below the Iberian Peninsula: Evidence for a subducted lithosphere beneath southern Spain, *Tectonophysics*, *221*, 13–34.

Bowin, C. (1991), The Earth's gravity field and plate tectonics, *Tectonophysics*, *187*, 69–89.

Brede, R., M. Hauptmann, and H.-G. Herbig (1992), Plate tectonics and intracontinental mountain ranges in Morocco—The Mesozoic-Cenozoic development in the central High Atlas and the Middle Atlas, *Geol. Rundsch.*, *81*, 127–141.

Buforn, E., and P. Coca (2002), Seismic moment tensor for intermediate depth earthquakes at regional distances in Southern Spain, *Tectonophysics*, *356*, 49–63.

Calvert, A., E. Sandvol, D. Seber, M. Barazangi, S. Roecker, T. Mourabit, F. Vidal, G. Alguacil, and N. Jabour (2000), Geodynamic evolution of the lithosphere and upper mantle beneath the Alboran region of the western Mediterranean: Constraints from travel time tomography, *J. Geophys. Res.*, *105*, 10,871–10,899.

Carbonell, R., et al. (2003), Coincident magnetotelluric and deep seismic reflection sounding of a transpressive orogen: SW-Iberia, paper presented at 10th International Symposium on Deep Seismic Profiling of the Continents and Their Margins, Int. Assoc. of Seismol. and Phys. of the Earth's Inter., Taupo, New Zealand.

Charroud, M. (1990), Évolution géodynamique de la partie Sud-Ouest du Moyen-Atlas durant le passage Jurasique-Crétacé, le Crétacé et le Paléogène: Un example d'évolution intraplaque, Ph.D. thesis, Univ. Mohammed V, Rabat, Morocco.

Comas, M. C., J. J. Dañobeitia, J. Álvarez-Marrón, and J. I. Soto (1997), Crustal reflections and structure in the Alboran Basin: Preliminary results of the ESCI-Alboran survey, *Rev. Soc. Geol. Esp.*, *8*, 529–542.

d'Acremont, E., S. Leroy, and E. B. Burov (2003), Numerical modelling of a mantle plume: The plume head-lithosphere interaction in the formation of an oceanic large igneous province, *Earth Planet. Sci. Lett.*, *206*, 379–396.

Dañobeitia, J. J., R. Bartolomé, A. Checa, A. Maldonado, and A. P. Slootweg (1999), An interpretation of a prominent magnetic anomaly near the boundary between the Eurasian and African plates (Gulf of Cadiz, SW margin of Iberia), *Mar. Geol.*, *155*, 45–62.

Dewey, J. F. (1988), Extensional collapse of orogens, *Tectonics*, *7*, 1123–1139.

Doblas, M., and R. Oyarzun (1989), Neogene extensional collapse in the western Mediterranean (Betic-Rif Alpine belt): Implications for the genesis of the Gibraltar Arc and magmatic activity, *Geology*, *17*, 430–433.

Docherty, C., and E. Banda (1995), Evidence for the eastward migration of the Alboran Sea based on regional subsidence analysis: A case for basin formation by delamination of the subcrustal lithosphere, *Tectonics*, *14*, 804–818.

Fernàndez, M., I. Marzán, A. Correia, and E. Ramalho (1998), Heat flow, heat production and lithospheric thermal regime in the Iberian Peninsula, *Tectonophysics*, *291*, 29–53.

Fernàndez, M., I. Marzan, and M. Torne (2004), Lithospheric transition from the Variscan Iberian Massif to the Jurassic oceanic crust of the Central Atlantic, *Tectonophysics*, *386*, 97–115.

Flinch, J. F., A. W. Bally, and S. Wu (1996), Emplacement of a passive-margin evaporitic allochthon in the Betic Cordillera of Spain, *Geology*, *24*, 67–70.

Frizon de Lamotte, D., B. Saint Bézar, R. Bracène, and E. Mercier (2000), The two main steps of the Atlas building and geodynamics of the western Mediterranean, *Tectonics*, *19*, 740–761.

Froitzheim, N., N. Stets, and P. Wurster (1988), Aspects of western High Atlas tectonics, in *The Atlas System of Morocco*, edited by V. Jacobshagen, pp. 219–244, Springer, New York.

Galdeano, A., V. Courtillot, E. Le Borgne, J. L. Le Mouël, and J. C. Rossignol (1974), An aeromagnetic survey of the southwest of the western Mediterranean: Description and tectonic implications, *Earth Planet. Sci. Lett.*, *23*, 323–336.

Gómez, F., R. Allmendinger, M. Barazangui, A. Er-Raji, and M. Dahmani (1998), Crustal shortening and vertical strain partitioning in the Middle Atlas mountains of Morocco, *Tectonics*, *17*, 520–533.

González, A., M. Torné, D. Córdoba, N. Vidal, L. M. Matias, and J. Díaz (1996), Crustal thinning in the southwestern Iberian Margin, *Geophys. Res. Lett.*, *23*, 2477–2480.

González, A., D. Córdoba, R. Vegas, and L. M. Matias (1998), Seismic crustal structure in the southwest of the Iberian Peninsula and the Gulf of Cadiz, *Tectonophysics*, *296*, 317–331.

Gràcia, E., J. Dañobeitia, J. Vergés, R. Bartolomé, and D. Córdoba (2003), Crustal architecture and tectonic evolution of the Gulf of Cadiz (SW Iberian margin) at the convergence of the Eur-

asian and African plates, *Tectonics*, *22*(4), 1033, doi:10.1029/2001TC901045.
Granet, M., G. Stoll, J. Dorel, U. Achauer, J. Poupinet, and K. Fuchs (1995), Massif Central (France): New constraints on the geodynamical evolution from teleseismic tomography, *Geophys. J. Int.*, *121*, 33–48.
Gutscher, M.-A., J. Malod, J.-P. Rehault, I. Contrucci, F. Klingelhoefer, L. Mendes-Victor, and W. Spakman (2002), Evidence for active subduction beneath Gibraltar, *Geology*, *30*, 1071–1074.
Hammond, W. C., and E. D. Humphreys (2000a), Upper mantle seismic wave attenuation: Effects of realistic partial melt distribution, *J. Geophys. Res.*, *105*, 10,987–11,000.
Hammond, W. C., and E. D. Humphreys (2000b), Upper mantle seismic wave velocity: Effects of realistic partial melt geometries, *J. Geophys. Res.*, *105*, 10,975–10,986.
Harmand, C., and J. M. Cantagrel (1984), Le volcanisme alcalin Tertiaire et Quaternaire du Moyen Atlas (Maroc): Chronologie K/Ar et cadre geodynamique, *J. Afr. Earth Sci.*, *2*, 51–55.
Harmand, C., and A. Moukadiri (1986), Synchronisme entre tectonique compressive et volcanisme alcalin: Exemple de la province quaternaire du Moyen Atlas (Maroc), *Bull. Soc. Geol. Fr.*, *1986*, 595–603.
Hatzfeld, D., and M. Frogneaux (1981), Intermediate depth seismicity in the western Mediterranean unrelated to subduction of oceanic lithosphere, *Nature*, *292*, 443–445.
Hatzfeld, D., et al. (1978), Crustal seismic profiles in the Alboran Sea: Preliminary results, *Pure Appl. Geophys.*, *116*, 167–180.
Herbig, H.-G. (1988), Synsedimentary tectonics in the northern Middle Atlas (Morocco) during the Late Cretaceous and Tertiary, in *The Atlas System of Morocco: Studies on Its Geodynamic Evolution*, *Lecture Notes Earth Sci.*, vol. 15, edited by V. H. Jacobshagen, pp. 321–337, Springer, New York.
Hildenbrand, T., R. Kucks, M. Hamouda, and A. Bellot (1988), Bouguer gravity map and related filtered anomaly maps of Morocco, 15 pp., U.S. Geol. Surv., Denver, Colo.
Hoernle, K., Y. S. Zhang, and D. Graham (1995), Seismic and geochemical evidence for large-scale mantle upwelling beneath the eastern Atlantic and western and central Europe, *Nature*, *374*, 34–39.
ILIHA DSS Group (1993), A deep seismic sounding investigation of lithospheric heterogeneity and anisotropy beneath the Iberian Peninsula, *Tectonophysics*, *221*, 35–51.
Jacobshagen, V., K. Görler, and P. Giese (1988), Geodynamic evolution of the Atlas system (Morocco) in post-Paleozoic times, in *The Atlas System of Morocco: Studies on Its Geodynamic Evolution*, *Lecture Notes Earth Sci.*, vol. 15, edited by V. H. Jacobshagen, pp. 481–499, Springer, New York.
Klitgord, K. D., and H. Schouten (1986), Plate kinematics of the central Atlantic, in *The Geology of North America*, vol. M, *The Western North Atlantic Region*, edited by P. R. Vogt and B. E. Tucholke, pp. 351–378, Geol. Soc. of Am., Boulder, Colo.
Lachenbruch, A. H., and P. Morgan (1990), Continental extension, magmatism and elevation: Formal relations and rules of thumb, *Tectonophysics*, *174*, 39–62.
Laville, E., and J. P. Petit (1984), Role of synsedimentary strike-slip faults in the formation of the Moroccan Triassic basins, *Geology*, *12*, 424–427.
Lee, C.-T. A. (2003), Compositional variation of density and seismic velocities in natural peridotites at STP conditions: Implications for seismic imaging of compositional heterogeneities in the upper mantle, *J. Geophys. Res.*, *108*(B9), 2441, doi:10.1029/2003JB002413.
Lemoine, F. G., et al. (1998), The development of the joint NASA GSFC and NIMA Geopotential Model EGM96, NASA Goddard Space Flight Cent., Greenbelt, Md.
Litto, W., E. B. Jaaidi, F. Medina, and M. Dakki (2001), Etude sismo-structurale de la marge nord du bassin du Gharb (avant-pays rifain, Maroc): Mise en évidence d'une distension d'âge miocène tardif, *Eclogae Geol. Helv.*, *94*, 63–73.
Lonergan, L., and N. White (1997), Origin of the Betic-Rif mountain belt, *Tectonics*, *16*, 504–522.
López Casado, C., C. Sanz de Galdeano, S. Molina Palacios, and J. Henares Romero (2001), The structure of the Alboran Sea: An interpretation from seismological and geological data, *Tectonophysics*, *338*, 79–95.
Makris, J., A. Demnati, and J. Klussmann (1985), Deep seismic soundings in Morocco and a crust and upper mantle model deduced from seismic and gravity data, *Ann. Geophys.*, *3*, 369–380.
Maldonado, A., L. Somoza, and L. Pallarés (1999), The Betic orogen and the Iberian-African boundary in the Gulf of Cadiz: Geological evolution (central North Atlantic), *Mar. Geol.*, *155*, 9–43.
Malod, J. A., and A. Mauffret (1990), Iberian plate motion during the Mesozoic, *Tectonophysics*, *184*, 261–278.
Malod, J. A., et al. (2003), Crustal structure of the Moroccan Margin from the SISMAR seismic survey, *Geophys. Res. Abstr.*, *5*, 11,188.
McKenzie, D., and C. Bowin (1976), The relationship between bathymetry and gravity in the Atlantic ocean, *J. Geophys. Res.*, *81*, 1903–1915.
Mezcua, J., and J. Rueda (1997), Seismological evidence for a delamination process in the lithosphere under the Alboran Sea, *Geophys. J. Int.*, *129*, F1–F8.
Mezcua, J., A. Gil, and R. Benarroch (1996), Estudio gravimétrico de la Península Ibérica y Baleares, 14 pp., Inst. Geogr. Nac., Madrid.
Morales, J., I. Serrano, A. Jabaloy, J. Galindo-Zaldivar, D. Zhao, F. Torcal, F. Vidal, and F. Gonzalez-Lodeiro (1999), Active continental subduction beneath the Betic Cordillera and the Alboran Sea, *Geology*, *27*, 735–738.
Piqué, A., M. Dahmani, D. Jeannette, and L. Bahi (1987), Permanence of structural lines in Morocco from Precambrian to present, *J. Afr. Earth Sci.*, *6*, 247–256.
Platt, J. P., and R. L. M. Vissers (1989), Extensional collapse of thickened continental lithosphere: A working hypothesis for the Alboran Sea and the Gibraltar Arc, *Geology*, *29*, 299–302.
Platt, J. P., S. Allerton, A. Kirker, C. Mandeville, A. Mayfield, E. S. Platzman, and A. Rimi (2003), The ultimate arc: Differential displacement, oroclinal bending, and vertical axis rotation in the External Betic-Rif arc, *Tectonics*, *22*(3), 1017, doi:10.1029/2001TC001321.
Pollack, H. N., S. J. Hurter, and J. R. Johnson (1993), Heat flow from the Earth's Interior: Analysis of the global data set, *Rev. Geophys.*, *31*, 267–280.
Polyak, B. G., et al. (1996), Heat flow in the Alboran Sea, western Mediterranean, *Tectonophysics*, *263*, 191–218.
Poudjom-Djomani, Y. H., S. Y. O'Reilly, W. L. Griffin, and P. Morgan (2001), The density structure of subcontinental lithosphere through time, *Earth Planet. Sci. Lett.*, *184*, 605–621.
Purdy, G. M. (1975), The eastern end of the Azores-Gibraltar plate boundary, *Geophys. J. R. Astron. Soc.*, *43*, 973–1000.
Ramdani, F. (1998), Geodynamic implications of intermediate-depth earthquakes and volcanism in the intraplate Atlas mountains (Morocco), *Phys. Earth Planet. Inter.*, *108*, 245–260.
Rimi, A. (1999), Mantle heat flow and geotherms for the main geologic domains in Morocco, *Int. J. Earth Sci.*, *88*, 458–466.
Rimi, A., A. Chalouan, and L. Bahi (1998), Heat flow in the southernmost part of the Mediterranean alpine system, the External Rif in Morocco, *Tectonophysics*, *285*, 135–146.
Ritter, J. R. R., M. Jordan, U. R. Christensen, and U. Achauer (2001), A mantle plume below the Eifel volcanic fields, Germany, *Earth Planet. Sci. Lett.*, *186*, 7–14.
Royden, L. H. (1993), Evolution of retreating subduction boundaries formed during continental collision, *Tectonics*, *12*, 629–638.
Sandvol, E., D. Seber, A. Calvert, and M. Barazangi (1998), Grid search modeling of receiver functions: Implications for crustal structure in the Middle East and North Africa, *J. Geophys. Res.*, *103*, 26,899–26,918.
Sandwell, D. T., and W. H. F. Smith (1997), Marine gravity from Geosat and ERS 1 satellite altimetry, *J. Geophys. Res.*, *102*, 10,039–10,054.
Sanz de Galdeano, C. (1990), Geologic evolution of the Betic Cordilleras in the western Mediterranean, Miocene to present, *Tectonophysics*, *172*, 107–119.
Sartori, R., L. Torelli, N. Zitellini, D. Peis, and E. Lodolo (1994), Eastern segment of the Azores-Gibraltar line (central-eastern Atlantic): An oceanic plate boundary with diffuse compressional deformation, *Geology*, *22*, 555–558.
Schwarz, G., F. Ramdani, and V. Rath (1992), Electrical resistivity structure of the eastern Moroccan Atlas System and its tectonic implications, *Geol. Rundsch.*, *81*, 221–235.
Seber, D., M. Barazangi, A. Ibenbrahim, and A. Demnati (1996a), Geophysical evidence for lithospheric delamination beneath the Alboran Sea and Rif-Betic mountains, *Nature*, *379*, 785–790.
Seber, D., M. Barazangi, B. A. Tadili, M. Ramadani, A. Ibenbrahim, and D. Ben Sari (1996b), Three-dimensional upper mantle structure beneath the intraplate Atlas and interplate Rif mountains of Morocco, *J. Geophys. Res.*, *101*, 3125–3138.
Seber, D., E. Sandvol, C. Sandvol, C. Brindisi, and M. Barazangi (2001), Crustal model for the Middle East and North Africa region: Implications for the isostatic compensation mechanism, *Geophys. J. Int.*, *147*, 630–638.
Service Géologique du Maroc (1985), Carte géologique du Maroc, 1:1,000,000, 2 sheets, Rabat, Morocco.
Simancas, J. F., et al. (2003), Crustal structure of the transpressional Variscan Orogen of SW Iberia: SW Iberia deep seismic reflection profile (IBERSEIS), *Tectonics*, *22*(6), 1062, doi:10.1029/2002TC001479.
Sobolev, S., H. Zeyen, G. Stoll, F. Werling, R. Altherr, and K. Fuchs (1996), Upper mantle temperatures from teleseismic tomography of French Massif Central including effects of composition, mineral reactions, anharmonicity, anelasticity and partial melt, *Earth Planet. Sci. Lett.*, *139*, 147–163.
Srivastaba, S. P., W. R. Roest, L. C. Kovacs, G. Oakey, S. Levesque, J. Verhoef, and R. Macnab (1990), Motion of Iberia since the Late Jurassic: Results from detailed aeromagnetic measurements in the Newfoundland Basin, *Tectonophysics*, *184*, 229–260.
Tadili, B., M. Ramdani, D. Ben Sari, K. Chapochnikov, and A. Bellot (1986), Structure de la croûte dans le nord du Maroc, *Ann. Geophys.*, *4*, 99–104.
Talwani, M., J. L. Worzel, and M. Landisman (1959), Rapid gravity computations for two-dimensional bodies with application to the Mendocino submarine fracture zone, *J. Geophys. Res.*, *64*, 49–59.
Teixell, A., M.-L. Arboleya, M. Julivert, and M. Charroud (2003), Tectonic shortening and topography in the central High Atlas (Morocco), *Tectonics*, *22*(5), 1051, doi:10.1029/2002TC001460.
Torné, M., and E. Banda (1992), Crustal thinning from the Betic Cordillera to the Alboran Sea, *Geo-Mar. Lett.*, *12*, 76–81.
Torné, M., M. Fernàndez, M. C. Comas, and J. I. Soto (2000), Lithospheric structure beneath the Alboran Basin: Results from 3D gravity modeling and tectonic relevance, *J. Geophys. Res.*, *105*, 3209–3228.
Torres-Roldan, R. L., G. Poli, and A. Peccerillo (1986), An early Miocene arc-tholeitic magmatic dyke event from the Alboran Sea: Evidence for precollision subduction and back-arc crustal extension in

the westernmost Mediterranean, *Geol. Rundsch.*, *75*, 219–234.

Tortella, D., M. Torné, and A. Pérez-Estaún (1997), Geodynamic evolution of the Eastern Segment of the Azores-Gibraltar Zone: The Gorringe Bank and the Gulf of Cadiz Region, *Mar. Geophys. Res.*, *19*, 211–230.

Turcotte, D. L., and G. Schubert (1982), *Geodynamics*, 450 pp., John Wiley, Hoboken, N. J.

van der Meijde, M., S. van der Lee, and D. Giardini (2003), Crustal structure beneath broad-band seismic stations in the Mediterranean region, *Geophys. J. Int.*, *152*, 729–739.

Watts, A. B., J. P. Platt, and P. Buhl (1993), Tectonic evolution of the Alboran Sea Basin, *Basin Res.*, *5*, 153–177.

Wigger, P., G. Asch, P. Giese, W.-D. Heinsohn, S. O. El Alami, and F. Ramdani (1992), Crustal structure along a traverse across the Middle and High Atlas Mountains derived from seismic refraction studies, *Geol. Rundsch.*, *81*, 237–248.

Zeck, H. P. (1997), Mantle peridotites outlining the Gibraltar Arc: Centrifugal extensional allochthonous derived from the earlier Alpine, westward subducted nappe pile, *Tectonophysics*, *281*, 195–207.

Zeyen, H., and M. Fernàndez (1994), Integrated lithospheric modeling combining thermal, gravity, and local isostasy analysis: Application to the NE Spanish Geotransect, *J. Geophys. Res.*, *99*, 18,089–18,102.

Zitellini, N., L. Mendes-Victor, D. Córdoba, J. J. Dañobeitia, R. Nicolich, G. Pellis, A. Ribeiro, R. Sartori, and L. Torelli (2001), Source of the 1755 Lisbon earthquake and tsunami investigated, *Eos Trans. AGU*, *82*, 285, 290–291.

Zouine, E. M. (1993), Géodynamique récente du Haut Atlas. Evolution de sa bordure septentrionale et du Moyen Atlas sud-occidental au cours du Cénozoïque, Ph.D. thesis, 303 pp., Univ. Mohammed V, Rabat.

P. Ayarza, Facultad de Ciencias, Departamento de Geologia, Universidad de Salamanca, E-37008 Salamanca, Spain.

M. Fernàndez, Group of Dynamics of the Lithosphere, Institute of Earth Sciences "Jaume Almera," Consejo Superior de Investigaciones Científicas (CSIC), Solé Sabarís s/n, E-08028 Barcelona, Spain.

A. Rimi, Scientific Institute, Department of Earth Physics, Chariá lbn Battouta, B.P. 703, Rabat-Agdal, Morocco.

H. Zeyen, Département des Sciences de la Terre, FRE 2566, Université Paris-Sud, Bât. 504, F-91405 Orsay cedex, France. (zeyen@geol.u-psud.fr)